

論文 / 著書情報  
Article / Book Information

Title	Mg <sub>x</sub> Zn <sub>1-x</sub> O as a II-VI widegap semiconductor alloy
Authors	A. Ohtomo, M. Kawasaki, T. Koida, K. Masubuchi, H. Koinuma, Y. Sakurai, Y. Yoshida, T. Yasuda, Y. Segawa
Citation	Applied Physics Letters, Vol. 72, No. 19,
Pub. date	1998, 5
URL	<a href="http://scitation.aip.org/content/aip/journal/apl">http://scitation.aip.org/content/aip/journal/apl</a>
Copyright	Copyright (c) 1998 American Institute of Physics

## Mg<sub>x</sub>Zn<sub>1-x</sub>O as a II–VI widegap semiconductor alloy

A. Ohtomo,<sup>a)</sup> M. Kawasaki, T. Koida, K. Masubuchi, and H. Koinuma<sup>b)</sup>  
*Tokyo Institute of Technology, 4259 Nagatsuda, Midori-ku, Yokohama 226, Japan*

Y. Sakurai and Y. Yoshida  
*Faculty of Engineering, Toyo University, 2100 Kujirai, Kawagoe 350, Japan*

T. Yasuda and Y. Segawa  
*Photodynamic Research Center, The Institute of Physical and Chemical Research, 19-1399 Nagamachi  
 Koeji, Aoba, Sendai 980, Japan*

(Received 8 December 1997; accepted for publication 12 March 1998)

We propose a widegap II–VI semiconductor alloy, Mg<sub>x</sub>Zn<sub>1-x</sub>O, for the fabrication of heteroepitaxial ultraviolet light emitting devices based on ZnO. The *c*-axis oriented Mg<sub>x</sub>Zn<sub>1-x</sub>O films were epitaxially grown by pulsed laser deposition on ZnO epitaxial films and sapphire (0001) substrates using ceramic targets. Solid solution films were prepared with Mg content up to  $x = 0.33$ , achieving a band gap of 3.99 eV at room temperature. MgO impurity phase segregated at  $x \geq 0.36$ . Lattice constants of Mg<sub>x</sub>Zn<sub>1-x</sub>O films changed slightly ( $\sim 1\%$ ), increasing in *a* axis and decreasing in *c*-axis direction with increasing *x*. These films showed ultraviolet photoluminescence at energies from 3.36 ( $x = 0$ ) to 3.87 eV ( $x = 0.33$ ) at 4.2 K. © 1998 American Institute of Physics. [S0003-6951(98)04219-3]

A heterojunction is one of the key structures for constructing various electronic and optical devices using compound semiconductors. Modulation of the band gap with keeping the lattice constants similar to each other is essential for this purpose. For instance, a double heterostructure (DH) composed of a thin well layer sandwiched between two barrier layers has been utilized in laser diodes to facilitate radiative recombination by carrier confinement.<sup>1</sup> We recently reported that stimulated emission due to excitonic recombination could be observed at room temperature by optically pumping ZnO nanocrystalline thin films epitaxially grown on sapphire substrates.<sup>2</sup> Laser action with a very low threshold intensity (24 kW/cm<sup>2</sup>) took place using naturally occurring grain boundaries as cavity mirrors.<sup>3</sup> For fabricating a DH laser diode using a ZnO active layer, two critical materials challenges are *p*-type doping<sup>4</sup> and band gap engineering in alloy semiconductors. We concentrate on the latter in this letter.

In case of ZnSe-based lasers, the Zn<sub>x</sub>Mg<sub>1-x</sub>S<sub>y</sub>Se<sub>1-y</sub> alloy with *x* up to 0.4 has been used for barrier and cladding layers.<sup>5</sup> Wide range solubility of Mg in the zinc blend structure was expected because the tetrahedral ionic radius of Mg<sup>2+</sup> (0.57 Å) is similar to that of Zn<sup>2+</sup> (0.60 Å).<sup>6</sup> Here, we propose a novel II–VI oxide semiconductor alloy system, Mg<sub>x</sub>Zn<sub>1-x</sub>O, which has excellent optical properties and similar lattice constants to those of ZnO.

Mg<sub>x</sub>Zn<sub>1-x</sub>O thin films were grown on sapphire (0001) substrates, polished on both sides, by pulsed laser deposition in an ultrahigh vacuum chamber.<sup>7</sup> Predetermined amounts of ZnO (5 N) and MgO (4 N) powders were mixed, calcined, and sintered to form targets with Mg content ranging from  $x = 0$  to  $x = 0.18$ . The x-ray diffraction (XRD) spectra of the targets showed no detectable MgO peaks for  $x \leq 0.10$ ,

whereas clear MgO peaks for  $x \geq 0.13$ . The targets were placed at a distance of 4 cm from the substrate and ablated by KrF excimer laser pulses (254 nm, 10 Hz, 20 ns) with a fluence of 1 J/cm<sup>2</sup>. The films ( $\sim 300$  nm thick) were deposited at a temperature of 600 °C in  $5 \times 10^{-5}$  Torr of pure oxygen (99.9999%). Mg content in the Mg<sub>x</sub>Zn<sub>1-x</sub>O films was determined by inductively coupled plasma (ICP) optical emission spectroscopy by dissolving the films in HNO<sub>3</sub> solution. The surface morphology of the films was examined by means of contact-mode atomic force microscopy (AFM). The crystal structure of the films was analyzed by  $\theta$ – $2\theta$  XRD and four-circle XRD (Philips, X' Pert-MRD) with a resolution of 0.005°. Out-of-plane and in-plane mosaicism were evaluated by setting the Bragg diffraction angle to the ZnO (0002) and (1 $\bar{1}$ 01) reflections, respectively, where  $\bar{1}$  stands for negative value of Miller index. Optical properties were characterized by absorption and photoluminescence spectroscopies. A continuous He–Cd laser (325 nm) and a pulsed XeCl excimer laser (308 nm, 10 Hz) were used for the photoluminescence measurements.

Deposition rate of the films was  $1.5 \times 10^{-2}$  nm/pulse regardless Mg content in the targets. Figure 1 shows the Mg content in the films as a function of that in the targets. The Mg content in the films was systematically larger than in the targets by a factor of 2.5. This difference can be attributed to the fact that the vapor pressure of ZnO and Zn is much larger than that of MgO and Mg at the substrate temperature.<sup>8</sup> Zn-related species can easily desorb from the growing surface and lead to the condensation of Mg-related species on the surface.

Single-phase thin films having wurtzite structure and *c*-axis orientation could be prepared with *x* up to 0.25, as verified by XRD analysis. When Mg content was larger than 0.36, small peaks due to an impurity phase [(111) oriented MgO] were observed. At  $x = 0.33$ , very weak signal could be detected where MgO(222) peak should appear. However the intensity was much smaller than ZnO(0002) peak by factor

<sup>a)</sup>Electronic mail: ohtomo@oxide.rlem.titech.ac.jp

<sup>b)</sup>Also a member of CREST, Japan Science & Technology Corporation.

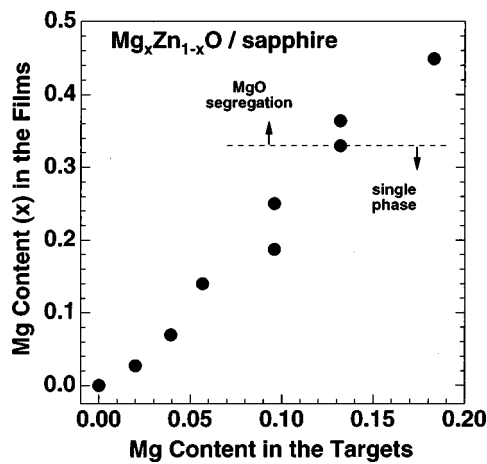


FIG. 1. Mg content in the  $Mg_xZn_{1-x}O$  epitaxial films as a function of target Mg content.

of  $10^{-4}$ , therefore, the solubility limit of MgO in ZnO for the films prepared in this study should be as large as 33 mol %. The thermodynamic solubility limit of MgO in ZnO has been reported to be less than 4 mol %, according to the phase diagram of the ZnO–MgO binary system.<sup>9</sup> The  $Mg_xZn_{1-x}O$  films reported here can therefore be considered as metastable phases. Pulsed laser deposition is a suitable growth method for fabricating such metastable phase films because of the high peak energy of the laser light. Target material is instantaneously evaporated during the laser pulses, providing gas phase precursors with a fairly high energy (several tens of eV).<sup>10</sup> The precursors arrive at the substrate surface and are rapidly cooled, crystallizing at the substrate temperature. The nonequilibrium nature of this crystal growth enabled us to fabricate solid solution films well above the thermodynamic solubility limit.

Lattice constants measured by the four-circle XRD are plotted as a function of the Mg content in Fig. 2. The *a*-axis length gradually increases, while the *c*-axis length decreases with increasing Mg content. Consequently, the cell volume  $[3\sqrt{3}/2a^2c]$  hardly changed, agreeing with the fact that ionic radii of  $Zn^{2+}$  and  $Mg^{2+}$  have similar values. Since the lattice constants still showed gradual change up to  $x=0.33$ , where impurity MgO phase started to appear in XRD, we can conclude that the solubility limit under these conditions was between  $x=0.25$  and  $0.33$ .

An in-plane (0002)  $\omega$  scan and an out-of-plane (1101)  $\phi$  scan of a  $x=0.19$  film are shown in Fig. 3. Full width at half maximum (FWHM) values of (0002) and (1101) rocking curves were  $0.13^\circ$  and  $0.55^\circ$ , respectively. These values are comparable to the highest quality pure ZnO films of about the same thickness prepared in our laboratory ( $0.12^\circ$  and  $0.51^\circ$ , respectively). The in-plane crystal orientation was determined to be  $Mg_xZn_{1-x}O(1\bar{1}00)\parallel\alpha-Al_2O_3(11\bar{2}0)$ , which is the same as that of ZnO/ $\alpha-Al_2O_3$  and GaN/ $\alpha-Al_2O_3$ .<sup>11</sup>

Figure 4 shows transmittance spectra measured at room temperature by conventional ultraviolet-visible spectrometer. As can be clearly seen, the absorption edge shifted as a function of  $x$  when  $x \leq 0.36$ , saturating at higher Mg concentration. These results are in good agreement with the appearance of the MgO impurity phase detected by XRD. For evaluating the band gap ( $E_g$ ), we employed an  $\alpha^2$  vs  $E_g$  plot

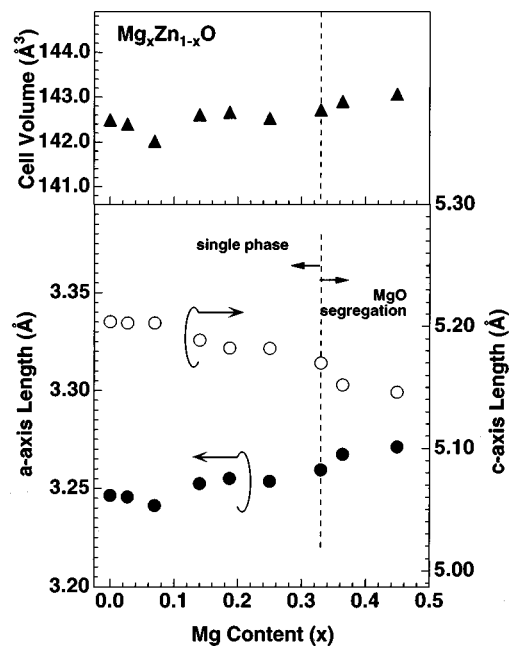


FIG. 2. Mg content dependences of the *a*- and *c*-axis lattice parameters and the cell volume of  $Mg_xZn_{1-x}O$  films. Segregation of the MgO impurity phase was observed for  $x \geq 0.33$  of Mg content.

for the spectra to fit the data assuming an  $\alpha^2 \propto (h\nu - E_g)$  relationship, where  $\alpha$  is the absorption coefficient and  $h\nu$  is the photon energy. The band gap is shown as a function of  $x$  in the inset of Fig. 4.  $E_g$  linearly increased up to 4.15 eV for  $0 \leq x \leq 0.36$ , indicating that the  $Mg_xZn_{1-x}O$  alloy is a suitable material for potential barrier layers in ZnO-based devices having the band gap offset as large as 0.85 eV.

Figure 5 shows photoluminescence and absorption spectra taken at 4.2 K of samples with  $x \leq 0.33$ , where single phase films could be grown. With increasing  $x$ , the luminescence peak shifted to higher energy. The luminescence peak of pure ZnO film ( $x=0$ ) had slightly lower energy than those of A and B exciton peaks clearly visible in the absorption spectrum.<sup>2</sup> This emission can be attributed to a bound exciton emission line (I), i.e., the recombination of excitons trapped in shallow impurity levels. The alloy film with  $x=0.03$  showed a luminescence peak at an energy close to the

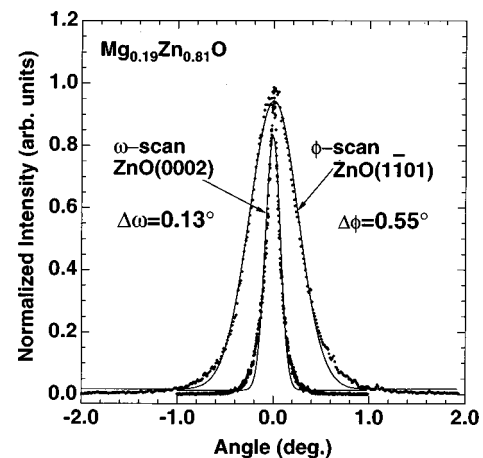


FIG. 3. X-ray diffraction rocking curves showing (0002)  $\omega$  and (1101)  $\phi$  scans of a  $Mg_{0.19}Zn_{0.81}O$  film. The width of the peaks are comparable to the highest quality pure ZnO films.

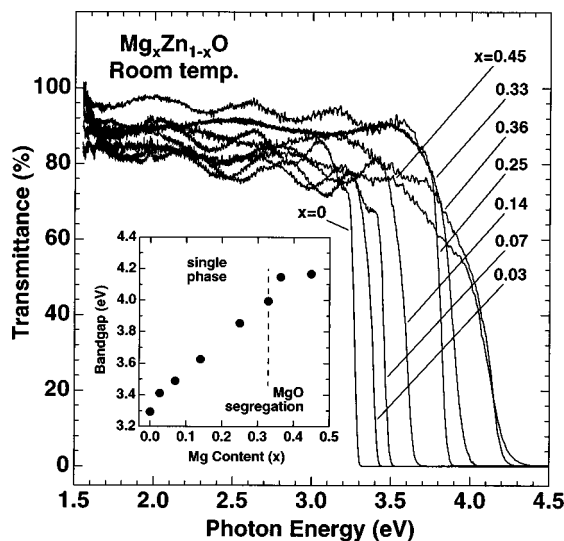


FIG. 4. Transmittance spectra of  $\text{Mg}_x\text{Zn}_{1-x}\text{O}$  films measured at room temperature. The inset shows the band gap ( $E_g$ ) determined from the spectra assuming an  $\alpha^2 \propto (h\nu - E_g)$  dependence, where  $\alpha$  and  $h\nu$  are the absorption coefficient and the photon energy, respectively.

absorption edge. This is probably due to the screening effect, where excitons are no longer trapped at intrinsic impurities because the Mg ions become the major impurity. When  $x \geq 0.07$ , the luminescence peaks showed Stokes shift to the lower energy side of the absorption edge. The broadening and Stokes shift of the luminescence peak are frequently ob-

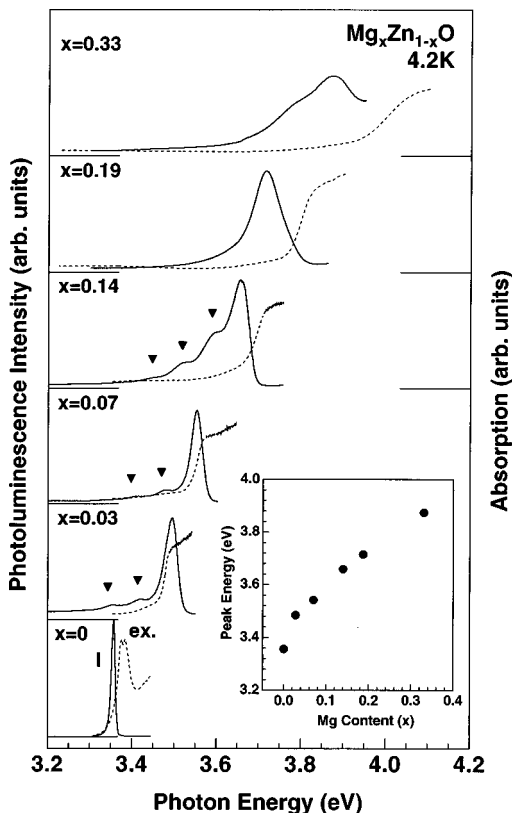


FIG. 5. Photoluminescence (solid lines) and absorption spectra (dotted lines) of  $\text{Mg}_x\text{Zn}_{1-x}\text{O}$  films ( $0 \leq x \leq 0.33$ ). The spectra were taken at 4.2 K. The inset shows the luminescence peak position as a function of Mg content. For the films with  $0 \leq x \leq 0.14$ , He-Cd laser excitation (3.81 eV) was employed. For the films with  $0.19 \leq x \leq 0.33$ , XeCl laser pulses (4.03 eV) were used. Solid triangles corresponded to the peaks due to phonon replicas.

served in alloy semiconductors,<sup>12</sup> where carriers feel different potentials depending on the local concentration and/or arrangement of the substituting elements. This effect is larger in ZnO than in III-V semiconductors, because the Bohr radius of excitons in ZnO is as small as 18 Å and the excitons are therefore more sensitive to local inhomogeneity. On the lower energy side of the emission peaks for  $x \leq 0.14$  samples, small peaks can be seen at a constant interval (about 70 meV) as denoted by filled triangles in Fig. 5. These peaks can be attributed to the LO-phonon replicas,<sup>13</sup> indicating high quality of the films in terms of crystallinity and optical properties. Thus,  $\text{Mg}_x\text{Zn}_{1-x}\text{O}$  films can be considered not only as barrier layers for the ZnO active layer, but also as an ultraviolet light emitting material, the luminescence energy of which can be tuned from 3.36 ( $x=0$ ) to 3.87 eV ( $x=0.33$ ) by adjusting the Mg content ( $x$ ).

For fabricating ZnO/ $\text{Mg}_x\text{Zn}_{1-x}\text{O}$  quantum well structures and superlattices, it is important to regulate the film surface and interface flatness. The alloy films deposited directly on sapphire had relatively rough surface compared to pure ZnO films. The root mean square (rms) roughness of the  $x=0.33$  film was 10 nm. The film with  $x \geq 0.36$  showed many particles on the surface probably due to MgO precipitates. However, by inserting a buffer ZnO film (100 nm), the surface of the alloy films ( $x \leq 0.33$ ) became as smooth as that of pure ZnO films and the rms value for roughness of the 300-nm-thick film was as small as 1 nm. This surface smoothness is acceptable for fabricating superlattices and quantum well structures.

In summary, we have fabricated  $\text{Mg}_x\text{Zn}_{1-x}\text{O}$  films by pulsed laser deposition. The optical band gap and photoluminescence peak can be tuned to the larger energy side while maintaining high crystallinity and without significant change of the lattice constants.

A.O. is supported by JSPS Research Fellowships for Young Scientists. This work was partly supported by JSPS Research for the Future Program in the area of Atomic-Scale Surface and Interface Dynamics (RFTF96P00205). The authors thank H. Imai of Asahi Chemical Industry Co., Ltd. for  $\mu$ -Auger measurement.

<sup>1</sup>I. Hayashi, M. B. Panish, P. W. Foy, and S. Sumski, Appl. Phys. Lett. **17**, 109 (1970).

<sup>2</sup>Z. K. Tang, P. Yu, G. K. L. Wong, M. Kawasaki, A. Ohtomo, H. Koinuma, and Y. Segawa, Solid State Commun. **103**, 459 (1997).

<sup>3</sup>Y. Segawa, A. Ohtomo, M. Kawasaki, H. Koinuma, Z. K. Tang, P. Yu, and G. K. L. Wong, Phys. Status Solidi B **202**, 669 (1997).

<sup>4</sup>K. Minegishi, Y. Koiwai, Y. Kikuchi, K. Yano, M. Kasuga, and A. Shimizu, Jpn. J. Appl. Phys., Part 2 **36**, L1453 (1997); J. T. Cheung (private communication).

<sup>5</sup>H. Okuyama, K. Nakano, T. Miyajima, and K. Akimoto, Jpn. J. Appl. Phys., Part 2 **30**, L1620 (1991).

<sup>6</sup>R. D. Shannon, Acta Crystallogr., Sect. A: Cryst. Phys., Diffr., Theor. Gen. Crystallogr. **32**, 751 (1976).

<sup>7</sup>H. Koinuma, M. Kawasaki, and M. Yoshimoto, Mater. Res. Soc. Symp. Proc. **397**, 145 (1996).

<sup>8</sup>R. E. Honig and D. A. Kramer, RCA Rev. **30**, 285 (1969).

<sup>9</sup>J. F. Sarver, Fred L. Katnack, and F. A. Hummel, J. Electrochem. Soc. **106**, 960 (1959).

<sup>10</sup>R. E. Leuchtner, Mater. Res. Soc. Symp. Proc. **397**, 157 (1996).

<sup>11</sup>M. Sano and M. Aoki, Jpn. J. Appl. Phys. **15**, 1943 (1976).

<sup>12</sup>For example, R. Zimmermann, J. Cryst. Growth **101**, 346 (1990).

<sup>13</sup>E. C. Heltemes and H. L. Swinney, J. Appl. Phys. **38**, 2387 (1967).